environmental and earth sciences proceedings

MDPI

Proceeding Paper

Granger Causality Analysis of Air Pollutants and Meteorological Parameters †

Wong Yee Ping [1], Zulkifli Abd Rais [1], Norazrin Ramli [1,2,*], Norazian Mohamed Noor [1,2], Ahmad Zia Ul-Saufie [3], Hazrul Abdul Hamid [4] and Mohd Khairul Nizam Mahmad [5]

1 Faculty of Civil Engineering & Technology, Universiti Malaysia Perlis, Jejawi, Arau 02600, Perlis, Malaysia; s201132003@studentmail.unimap.edu.my (W.Y.P.); zulkiflirais@studentmail.unimap.edu.my (Z.A.R.); norazian@unimap.edu.my (N.M.N.)
2 Sustainable Environment Research Group (SERG), Centre of Excellence Geopolymer and Green Technology (CEGeoGTech), Universiti Malaysia Perlis, Jejawi, Arau 02600, Perlis, Malaysia
3 Faculty of Computer and Mathematical Sciences, Universiti Teknologi Mara (UiTM), Shah Alam 40450, Selangor, Malaysia; ahmadzia101@uitm.edu.my
4 School of Distance Education, Universiti Sains Malaysia, Gelugor 11800, Penang, Malaysia; hazrul@usm.my
5 Mining and Energy Resources Academy (MERA), Jalan Kuala Ketil, Parit Panjang, Baling 09100, Kedah, Malaysia; nizam.mahmad@gmail.com
* Correspondence: norazrin@unimap.edu.my
† Presented at the 6th International Conference on Green Environmental Engineering and Technology (IConGEET2024), Bali, Indonesia, 29–30 August 2024.

Abstract: This study investigated the relationships between air pollutants (PM_{10}, SO_2, NO_2, O_3, CO) and meteorological parameters (wind speed, relative humidity, ambient temperature) across urban, suburban, and industrial areas in Malaysia from 2017 to 2021. Using data from six monitoring stations, this research employed descriptive analysis, trend analysis, and Granger causality testing to uncover complex interactions. The results revealed distinct patterns: suburban areas showed strong ambient temperature-ozone (p-value = 0.0063) and relative humidity–nitrogen dioxide relationships (p-value = 0.0411); industrial zones exhibited bidirectional causality between SO_2 and PM_{10} and had a strong nitrogen dioxide–PM_{10} relationship (p-value = 0.0292); urban areas exhibited complex multi-pollutant interactions. Notably, the 2020 Movement Control Order significantly improved air quality. This research provides crucial insights for targeted air quality management strategies, contributing to public health improvements and aligning with global sustainability goals.

Keywords: air pollutant; causality; Granger

check for updates

Academic Editor: Sara Yasina Yusuf

Published: 6 March 2025

Citation: Ping, W.Y.; Abd Rais, Z.; Ramli, N.; Mohamed Noor, N.; Ul-Saufie, A.Z.; Hamid, H.A.; Mahmad, M.K.N. Granger Causality Analysis of Air Pollutants and Meteorological Parameters. *Environ. Earth Sci. Proc.* **2025**, *33*, 6. https://doi.org/10.3390/eesp2025033006

1. Introduction

Air pollution is a critical environmental concern with significant impacts on human health, ecosystems, and climate change. In Malaysia, rapid industrialization, urbanization, and increasing vehicular emissions have contributed to deteriorating air quality, particularly in urban and industrial areas [1,2]. The complex interplay between air pollutants and meteorological parameters plays a crucial role in determining air quality, necessitating a comprehensive understanding of their relationships to develop effective mitigation strategies.

Extensive research has been conducted to explore the relationships between air pollutants and meteorological parameters. Studies have consistently shown that meteorological conditions significantly impact air quality fluctuations [3]. Wind speed affects the dispersion and transport of air pollutants, with higher wind speeds generally leading to lower pollutant concentrations [4]. Temperature variations influence chemical reactions and physical processes that determine pollutant concentrations in the atmosphere [5]. Relative humidity impacts the formation and transformation of certain pollutants, affecting overall air quality [6].

Existing studies [7,8] are limited by their regional focus, short-term scope, and lack of comprehensive data integration. While numerous studies [7–9] have employed correlation analysis to investigate these relationships, this approach has limitations. Correlation analysis assumes linear associations between variables and may not capture non-linear relationships [7]. Additionally, it is sensitive to extreme values and cannot establish causal relationships [8,9]. These limitations highlight the need for more advanced analytical approaches to understand the complex dynamics of air pollution.

To address these limitations and gain deeper insights into the cause-and-effect relationships between air pollutants and meteorological parameters, this study employs Granger causality analysis. Granger causality, a statistical concept developed by Nobel laureate Clive Granger, allows for the inference of causal relationships between variables based on time series data [10]. This approach has been successfully applied in various environmental studies to unravel complex interactions between different variables [11].

There are two main objectives in this study. Firstly, it aims to analyze the trends and characteristics of five key air pollutants—PM_{10}, NO_2, SO_2, O_3, and CO—alongside critical meteorological parameters such as wind speed, relative humidity, and ambient temperature. This analysis was conducted using data collected from selected monitoring stations across Malaysia between the years 2017 and 2021. Secondly, this study seeks to illustrate and interpret the Granger causality relationships between these air pollutants and meteorological parameters. This was achieved using graphical representations of causality, providing a visual and analytical understanding of the complex interactions between air quality and meteorological conditions. This study supports the UN's Sustainable Development Goal 11, aiming to reduce cities' environmental impacts by enhancing air quality.

2. Materials and Methods

This study used a data-driven approach to explore the relationships between air pollutants and weather conditions in Malaysia from 2017 to 2021. It involved three key phases: collecting and preprocessing data from six air quality monitoring stations, analyzing the temporal trends and stationarity of these data, and conducting Granger causality tests to understand the cause-and-effect dynamics between pollutants and meteorological factors.

2.1. Data Collection and Preliminary Data Processing

This study utilized secondary data from the Department of Environment Malaysia, covering 2017–2021. Data from six air quality monitoring stations (Table 1), representing urban, suburban, and industrial areas, included five air pollutants (PM_{10}, SO_2, NO_2, O_3, CO) and three meteorological parameters (wind speed, ambient temperature, relative humidity). Descriptive analysis using SPSS software version 27 (IBM SPSS Statistics 27) computed key statistical metrics (minimum, maximum, mean, standard deviation, skewness, kurtosis) for each parameter at each station, providing a comprehensive understanding of data characteristics and potential trends [12].

Table 1. The monitoring stations.

Station Id	Location	Longitude	Latitude	Category
CA31J	Batu Pahat, Johor	102.866618	1.919323	Sub Urban
CA33J	Larkin, Johor	103.735975	1.494625	Urban
CA35J	Pengerang, Johor	104.149586	1.389489	Industry
CA38C	Temerloh, Pahang	102.376406	3.471603	Sub Urban

Table 1. *Cont.*

Station Id	Location	Longitude	Latitude	Category
CA41C	Balok Baru Kuantan, Pahang	103.382158	3.960644	Industry
CA44T	Kuala Terengganu, Terengganu	103.120392	5.308094	Urban

2.2. Time Series Analysis and Stationarity Testing

The augmented Dickey–Fuller (ADF) test was employed using EViews software (11 Student Version) to examine data stationarity [13]. The test was conducted on the level form of each series, including trend and intercept. For *p*-values exceeding 0.05, indicating non-stationarity, data differencing was performed [14]. This process of differencing and retesting continued iteratively until stationarity was achieved, ensuring the data met assumptions for subsequent causality testing. This approach allowed for robust time series analysis, accounting for potential unit roots and non-stationary behavior in the data.

2.3. Granger Causality Analysis

The final phase of the methodology involved conducting Granger causality tests to explore the causal relationships between air pollutants and meteorological parameters. Prior to the causality analysis, the optimal lag length was determined using the Akaike information criterion (AIC) in EViews, striking a balance between model complexity and the goodness of fit [15]. The unrestricted vector autoregression (VAR) model was then estimated using the selected lag order. Granger causality tests were performed to assess whether the past values of one variable contained information that helped predict the future values of another variable [16]. The null hypothesis of no Granger causality was rejected if the *p*-value was less than or equal to 0.05, indicating a significant causal relationship [17]. The results of these tests were used to create graphical representations illustrating the direction and strength of the causal relationships between air pollutants and meteorological parameters across the monitoring stations.

3. Results and Discussion

3.1. Descriptive Analysis

The descriptive analysis of air pollutants and meteorological parameters across various Malaysian locations revealed distinct patterns and variations. Tables 2–9 are the descriptive analysis summary of air pollutant and meteorological parameters across urban, suburban, and industrial areas in Malaysia from 2017 to 2021.

Table 2. The PM_{10} concentration for all the monitoring stations.

Monitoring Stations	N	Minimum (μg/m^3)	Maximum (μg/m^3)	Mean (μg/m^3)	Std. Deviation	Skewness	Kurtosis
Batu Pahat, Johor (Sub Urban)	54	14.0730	67.4760	22.7603	8.7790	2.9855	12.6467
Larkin, Johor (Urban)	54	17.5910	72.5080	28.1959	8.3331	3.0072	14.3675
Pengerang, Johor (Industry)	54	11.3510	49.5800	20.9105	7.5007	1.3487	2.6379
Temerloh, Pahang (Sub Urban)	54	16.6130	68.0430	26.4649	8.4562	2.7191	10.8538

Table 2. *Cont.*

Monitoring Stations	N	Minimum ($\mu g/m^3$)	Maximum ($\mu g/m^3$)	Mean ($\mu g/m^3$)	Std. Deviation	Skewness	Kurtosis
Balok Baru Kuantan, Pahang (Industry)	54	15.6570	57.4890	27.5794	8.3385	1.4934	2.5762
Kuala Terengganu, Terengganu (Urban)	54	14.9940	51.8590	25.2872	6.7048	1.7135	4.5587

Table 3. The SO_2 concentration for all the monitoring stations.

Monitoring Stations	N	Minimum (ppm)	Maximum (ppm)	Mean (ppm)	Std. Deviation	Skewness	Kurtosis
Batu Pahat, Johor (Sub Urban)	54	0.0006	0.0021	0.0015	0.0003	−0.4059	−0.2356
Larkin, Johor (Urban)	54	0.0007	0.0032	0.0017	0.0005	0.0198	0.2661
Pengerang, Johor (Industry)	54	0.0007	0.0040	0.0014	0.0005	3.0120	14.0370
Temerloh, Pahang (Sub Urban)	54	0.0005	0.0013	0.0009	0.0002	0.4583	−0.0498
Balok Baru Kuantan, Pahang (Industry)	54	0.0006	0.0082	0.0013	0.0012	4.5445	22.0907
Kuala Terengganu, Terengganu (Urban)	54	0.0004	0.0016	0.0009	0.0003	0.6705	0.0723

Table 4. The NO_2 concentration for all the monitoring stations.

Monitoring Stations	N	Minimum (ppm)	Maximum (ppm)	Mean (ppm)	Std. Deviation	Skewness	Kurtosis
Batu Pahat, Johor (Sub Urban)	54	0.0027	0.0086	0.0050	0.0012	0.4650	0.7270
Larkin, Johor (Urban)	54	0.0039	0.0183	0.0115	0.0034	0.0484	−0.7534
Pengerang, Johor (Industry)	54	0.0012	0.0089	0.0047	0.0021	0.4311	−0.7606
Temerloh, Pahang (Sub Urban)	54	0.0021	0.0060	0.0043	0.0007	−0.8736	1.4554
Balok Baru Kuantan, Pahang (Industry)	54	0.0030	0.0074	0.0050	0.0011	0.0041	−0.7417
Kuala Terengganu, Terengganu (Urban)	54	0.0022	0.0070	0.0049	0.0010	−0.4823	−0.1139

Table 5. The O_3 concentration for all the monitoring stations.

Monitoring Stations	N	Minimum (ppm)	Maximum (ppm)	Mean (ppm)	Std. Deviation	Skewness	Kurtosis
Batu Pahat, Johor (Sub Urban)	54	0.0090	0.0252	0.0173	0.0030	0.3709	0.9379
Larkin, Johor (Urban)	54	0.0089	0.0089	0.0089	0.0089	0.0089	0.0089
Pengerang, Johor (Industry)	NA	NA	NA	NA	NA	NA	NA

Table 5. *Cont.*

Monitoring Stations	N	Minimum (ppm)	Maximum (ppm)	Mean (ppm)	Std. Deviation	Skewness	Kurtosis
Temerloh, Pahang (Sub Urban)	54	0.0084	0.0084	0.0084	0.0084	0.0084	0.0084
Balok Baru Kuantan, Pahang (Industry)	NA	NA	NA	NA	NA	NA	NA
Kuala Terengganu, Terengganu (Urban)	54	0.0089	0.0089	0.0089	0.0089	0.0089	0.0089

Table 6. The CO concentration for all the monitoring stations.

Monitoring Stations	N	Minimum, ppm	Maximum, ppm	Mean, ppm	Std. Deviation	Skewness	Kurtosis
Batu Pahat, Johor (Sub Urban)	54	0.3560	0.3560	0.3560	0.3560	0.3560	0.3560
Larkin, Johor (Urban)	54	0.1890	0.1890	0.1890	0.1890	0.1890	0.1890
Pengerang, Johor (Industry)	NA	NA	NA	NA	NA	NA	NA
Temerloh, Pahang (Sub Urban)	54	0.3450	0.3450	0.3450	0.3450	0.3450	0.3450
Balok Baru Kuantan, Pahang (Industry)	NA	NA	NA	NA	NA	NA	NA
Kuala Terengganu, Terengganu (Urban)	54	0.3720	0.3720	0.3720	0.3720	0.3720	0.3720

Table 7. The wind speed descriptives for all the monitoring stations.

Monitoring Stations	N	Minimum (m/s)	Maximum (m/s)	Mean (m/s)	Std. Deviation	Skewness	Kurtosis
Batu Pahat, Johor (Sub Urban)	54	0.7998	1.4955	1.0363	0.1799	0.9587	0.1152
Larkin, Johor (Urban)	54	0.5948	1.6048	0.8857	0.2669	1.4139	1.1703
Pengerang, Johor (Industry)	54	0.5035	2.1442	0.9983	0.3267	1.1117	1.6327
Temerloh, Pahang (Sub Urban)	54	0.7409	3.6060	1.0697	0.6193	3.8501	13.7479
Balok Baru Kuantan, Pahang (Industry)	54	1.3973	2.8910	1.9301	0.3666	0.8335	0.0152
Kuala Terengganu, Terengganu (Urban)	54	1.0335	1.7061	1.2839	0.1400	0.7758	1.3005

Table 8. The relative humidity descriptives for all the monitoring stations.

Monitoring Stations	N	Minimum (%)	Maximum (%)	Mean (%)	Std. Deviation	Skewness	Kurtosis
Batu Pahat, Johor (Sub Urban)	54	79.45	88.46	85.12	2.2378	−0.8554	0.2478
Larkin, Johor (Urban)	54	77.25	89.28	84.39	2.9827	−0.7621	−0.2905

Table 8. *Cont.*

Monitoring Stations	N	Minimum (%)	Maximum (%)	Mean (%)	Std. Deviation	Skewness	Kurtosis
Pengerang, Johor (Industry)	54	76.96	89.71	84.89	2.7600	−0.6615	0.7275
Temerloh, Pahang (Sub Urban)	54	73.34	89.70	82.33	3.5734	−0.1929	−0.4104
Balok Baru Kuantan, Pahang (Industry)	54	76.44	88.30	83.04	2.3133	−0.5923	0.6297
Kuala Terengganu, Terengganu (Urban)	54	77.68	90.40	83.51	2.6553	0.4387	0.1062

Table 9. The ambient temperature for all the monitoring stations.

Monitoring Stations	N	Minimum (°C)	Maximum (°C)	Mean (°C)	Std. Deviation	Skewness	Kurtosis
Batu Pahat, Johor (Sub Urban)	54	24.7	27.4	26.4	0.5294	−0.7286	1.0439
Larkin, Johor (Urban)	54	26.1	28.9	27.6	0.5669	0.0864	0.2471
Pengerang, Johor (Industry)	54	24.2	27.9	26.5	0.8231	−0.3216	−0.1303
Temerloh, Pahang (Sub Urban)	54	25.2	28.2	26.9	0.7662	−0.3916	−0.5059
Balok Baru Kuantan, Pahang (Industry)	54	24.5	27.9	26.6	0.7003	−0.5205	0.5214
Kuala Terengganu, Terengganu (Urban)	54	25.1	28.7	26.9	0.9089	−0.0085	−0.6517

Larkin, Johor (Urban), recorded the highest mean PM_{10} concentration at 28.1959 $\mu g/m^3$, with a maximum value of 72.5080 $\mu g/m^3$. Batu Pahat, Johor (Sub Urban), had the highest standard deviation at 8.7790. This indicated that the PM_{10} measurements at this station deviated the most from their mean value compared to other stations. In contrast, Kuala Terengganu, Terengganu (Urban), had the lowest standard deviation at 6.7048. This meant that the PM_{10} measurements at this station were closest to their mean value relative to the other stations. Larkin, Johor (Urban), had both the highest skewness (3.0072) and the highest kurtosis (14.3675). The high skewness indicated that the distribution of PM_{10} concentrations at this station was more asymmetrical compared to others.

Larkin, Johor (Urban), recorded the highest mean SO_2 concentration at 0.0017 ppm, with a maximum value of 0.0032 ppm. Batu Pahat, Johor (Sub Urban), followed closely with a mean concentration of 0.0015 ppm. Temerloh, Pahang (Sub Urban), and Kuala Terengganu, Terengganu (Urban), had the lowest mean SO_2 concentrations at 0.0009 ppm. Temerloh's values ranged from 0.0005 ppm to 0.0013 ppm, while Kuala Terengganu's ranged from 0.0004 ppm to 0.0016 ppm. Batu Pahat, Johor (Sub Urban), was the only station with a negative skew (−0.4059) and negative kurtosis (−0.2356), indicating a slight tendency towards lower values and a flatter distribution compared to a normal distribution. In summary, Larkin, Johor, recorded the highest mean SO_2 concentration, while Temerloh, Pahang, and Kuala Terengganu, Terengganu, had the lowest concentration. Balok Baru, Kuantan, Pahang, showed the highest maximum concentration and variability. The industrial stations (Balok Baru and Pengerang) exhibited higher skewness and kurtosis values, indicating more asymmetrical distributions.

Larkin, Johor (Urban), recorded the highest mean NO_2 concentration at 0.0115 ppm, with the maximum value of 0.0183 ppm. This station also had the highest standard deviation at 0.0034, indicating significant fluctuations in NO_2 levels compared to all stations. Temerloh, Pahang (Sub Urban), had the highest kurtosis (1.4554), reflecting a slightly heavier tail than a normal distribution. Larkin, Johor (Urban), and Pengerang, Johor (Industry), had high negative kurtosis values of −0.7534 and −0.7606 respectively, indicating slightly lighter tails than a normal distribution. In summary, Larkin, Johor (Urban), had the highest mean NO_2 concentration and the highest variability in measurements. Temerloh, Pahang (Sub Urban), showed the lowest mean concentration and the lowest variability. The skewness and kurtosis values varied across stations, with Temerloh showing the highest kurtosis and the highest negative skewness.

Batu Pahat, Johor (Sub Urban), recorded the highest mean O_3 concentration at 0.0173 ppm, with a maximum value of 0.0252 ppm. Larkin, Johor (Urban), exhibited the highest standard deviation at 0.0036, indicating the highest variability in O_3 measurements among all stations. In contrast, Temerloh, Pahang (Sub Urban), had the lowest standard deviation at 0.0028, suggesting the lowest variability in its O_3 concentration. Regarding skewness, Larkin, Johor (Urban), had the highest value at 0.6749, indicating the most asymmetrical distribution. Temerloh, Pahang (Sub Urban), had the lowest skewness at 0.1927, suggesting a more symmetrical distribution of O_3 concentrations compared to other stations.

Larkin, Johor (Urban), recorded the highest mean CO concentration at 0.6016 ppm, with a maximum value of 0.9630 ppm, and exhibited the highest variability with a standard deviation of 0.2181. In contrast, Kuala Terengganu, Terengganu (Urban), and Batu Pahat, Johor (Sub Urban), had lower standard deviations of 0.081 and 0.097, respectively. Kuala Terengganu, Terengganu, and Batu Pahat, Johor, demonstrated lower variability compared to the other stations.

The data showed considerable variation in wind speed characteristics across the monitoring stations. Balok Baru, Kuantan, Pahang (Industry), recorded the highest mean wind speed at 1.9301 m/s, with a maximum value of 2.8910 m/s. In contrast, Larkin, Johor (Urban), had the lowest mean wind speed at 0.8857 m/s, with values ranging from 0.5948 m/s to 1.6048 m/s. Balok Baru, Kuantan, Pahang, experienced the highest average wind speeds, while Larkin, Johor, had the lowest. Temerloh, Pahang, demonstrated the most extreme statistical measures, with the highest variability, skewness, and kurtosis.

Batu Pahat, Johor (Sub Urban), recorded the highest mean relative humidity at 85%, with a maximum value of 88%. This station had the lowest standard deviation, indicating the least variation in humidity readings among all stations. Kuala Terengganu, Terengganu (Urban), had the highest maximum relative humidity at 90%. Temerloh, Pahang (Sub Urban), had the lowest mean relative humidity at 82%, with values ranging from 73% to 89%. This station exhibited the highest variability, with a standard deviation of 3.57, indicating the largest spread of humidity readings.

Regarding skewness, Batu Pahat, Johor (Sub Urban), showed the highest negative skewness (−0.8554). Kuala Terengganu, Terengganu (Urban), was the only station with a positive skewness (0.4387). For kurtosis, Pengerang, Johor (Industry), indeed had the highest value (0.7275), indicating its humidity distribution had slightly heavier tails and a higher peak compared to a normal distribution. Larkin, Johor (Urban), had the lowest kurtosis (−0.2905), suggesting its humidity distribution had slightly lighter tails and a flatter peak compared to a normal distribution. Batu Pahat, Johor, recorded the highest mean relative humidity with the least variation, while Temerloh, Pahang, had the lowest mean and highest variability in relative humidity. Kuala Terengganu, Terengganu, reached the highest maximum humidity and was the only station with a positive skew in its readings. The humidity readings from Pengerang, Johor, showed the highest kurtosis, while those from Larkin, Johor, showed the lowest.

Larkin, Johor (Urban), recorded the highest mean ambient temperature at 27.6 °C, with the highest maximum value of 28.9 °C. Batu Pahat, Johor (Sub Urban), had the lowest mean ambient temperature at 26.4 °C, with values ranging from 24.7 °C to 27.4 °C. Kuala Terengganu, Terengganu (Urban), exhibited the highest variability with a standard deviation of 0.90, indicating there was a large spread of temperature values around its mean. In contrast, Batu Pahat, Johor (Sub Urban), had the lowest standard deviations (0.53), suggesting its temperature readings were more clustered around the mean.

In summary, urban areas, particularly Larkin, Johor, exhibited consistently higher mean concentrations for most air pollutants (PM_{10}, SO_2, NO_2, O_3, and CO) and often demonstrated the most skewed distributions, indicating significant air quality challenges. Conversely, suburban areas like Temerloh, Pahang, generally displayed lower mean pollutant concentrations, suggesting better air quality. Meteorological parameters showed diverse trends: Balok Baru Kuantan, Pahang, recorded the highest mean wind speed, while Larkin, Johor, experienced the lowest. Relative humidity was highest in Batu Pahat, Johor, which also exhibited the most skewed distribution for this parameter. There were ambient temperature peaks in Larkin, Johor, underscoring the urban heat island effect. The analysis indicated that pollutant levels and meteorological conditions varied significantly across urban, suburban, and industrial areas, with urban zones typically experiencing higher pollutant concentrations and temperatures. These findings highlight the complex interplay between urbanization, industrial activity, and environmental parameters, providing valuable insights for air quality management and urban planning strategies in Malaysia.

3.2. Trend Analysis

From 2017 to 2021, air quality in Malaysia generally remained within acceptable limits, which is the Air Pollutant Index (API) between 0–100, with occasional fluctuations influenced by seasonal and human factors. PM_{10} levels were mostly good to moderate, with a significant spike during the 2019 haze episode and a notable decrease during the 2020 MCO (first implemented in March 2020). The SO_2 concentration (24 h average: below 0.04 ppm), NO_2 concentration (24 h average: below 0.04 ppm), and CO concentration (8 h average: below 8.75 ppm) remained consistently low, well below MAAQG limits. O_3 levels, while within limits, were identified as a pollutant of concern. Meteorological parameters showed clear seasonal patterns: wind speeds increased during monsoons, particularly at coastal stations (Kuala Terengganu, Terengganu); relative humidity remained high (80–90%) with slight decreases during the Northeast Monsoon; and ambient temperatures fluctuated seasonally, with higher temperatures during the Southwest Monsoon, occurring from late May or early June to September, and lower during the Northeast Monsoon, occurring from November to March.

The impact of the Southwest Monsoon is that the coastal areas and islands on the west coast of Peninsular Malaysia experience less rainfall during this period, and weather conditions are generally dry for most parts of Malaysia. The Northeast Monsoon is characterized by heavy rainfall, especially along the east coast of Peninsular Malaysia and parts of Sabah and Sarawak. This monsoon often leads to frequent and intense rainstorms and sometimes even flooding in areas like Kelantan, Terengganu, and Pahang. Monsoonal patterns play a crucial role in air quality studies due to their significant influence on atmospheric conditions such as wind direction, ambient temperature, and humidity. These factors directly affect the dispersion, concentration, and transport of air pollutants. Understanding how these seasonal wind and weather systems affect pollutant behavior is critical for effective air quality management, pollution control policies, and public health protection.

The 2020 MCO period saw significant improvements in air quality across all pollutants due to reduced human activities. The Movement Control Order (MCO) implemented in Malaysia during 2020 in response to the COVID-19 pandemic had a profound impact on air quality, with significant improvements observed across multiple pollutants. This was primarily due to the drastic reduction in human activities, including transportation, industrial operations, and commercial activities, all of which are major sources of air pollution.

3.3. Dickey–Fuller Test Analysis

The Dickey–Fuller test results indicated varying levels of stationarity across different environmental parameters at the monitoring stations in Malaysia. For Batu Pahat, Johor, parameters such as PM_{10}, SO_2, NO_2, relative humidity (RH), and ambient temperature (AT) showed stationarity at level, while O_3, CO, and wind speed (WS) required first differencing. In Pengerang, Johor, PM_{10}, SO_2, WS, and AT were stationary at level, whereas NO_2 and RH needed first differencing. Larkin, Johor, saw many parameters like PM_{10}, SO_2, NO_2, and AT stationary at level, with O_3, CO, WS, and RH requiring first differencing. Temerloh, Pahang, exhibited stationarity at level for PM_{10}, NO_2, O_3, and CO, while SO_2, WS, RH, and AT needed first differencing. In Balok Baru Kuantan, Pahang, SO_2 and NO_2 were stationary at level, with PM_{10}, WS, RH, and AT requiring first differencing. Finally, Kuala Terengganu, Terengganu, had PM_{10}, SO_2, NO_2, O_3, CO, WS, and RH stationary at level, while AT needed first differencing. These results (Tables 10 and 11) demonstrate the dynamic nature of environmental data, influenced by local activities and climatic conditions, necessitating appropriate time series models for effective forecasting and analysis.

Table 10. The resulting Granger causality diagram for all the monitoring stations.

Monitoring Stations	Granger Causality Diagram
Batu Pahat, Johor (Sub Urban)	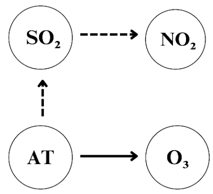
Pengerang, Johor (Industry)	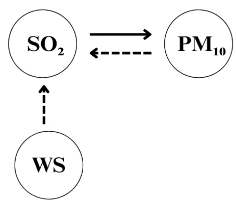
Larkin, Johor (Urban)	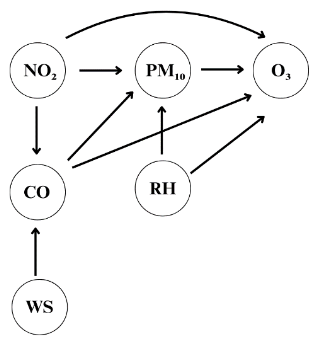

Table 10. *Cont.*

Monitoring Stations	Granger Causality Diagram
Temerloh, Pahang (Sub Urban)	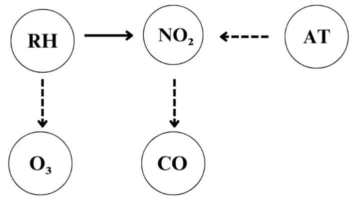
Balok Baru Kuantan, Pahang (Industry)	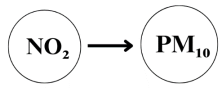
Kuala Terengganu, Terengganu (Urban)	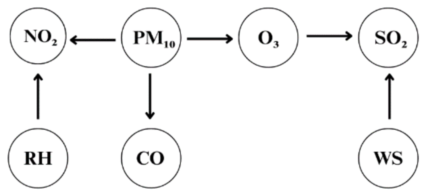

Solid lines indicate causality relationships with *p*-values less than 0.05. Dashed lines represent relationships with *p*-values between 0.05 and 0.10.

Table 11. The significant results from the Granger causality test for all the monitoring stations.

Monitoring Stations	Parameters	*p*-Value
Batu Pahat, Johor (Sub Urban)	Dependent parameter: SO_2 Independent parameter: AT	0.0733 **
	Dependent parameter: NO_2 Independent parameter: SO_2	0.0856 **
	Dependent parameter: O_3 Independent parameter: AT	0.0063 *
Pengerang, Johor (Industry)	Dependent parameter: PM_{10} Independent parameter: SO_2	0.0305 *
	Dependent parameter: SO_2 Independent parameter: PM_{10}	0.0994 **
	Dependent parameter: SO_2 Independent parameter: WS	0.0814 **
	Dependent parameter: NO_2 Independent parameter: RH	0.0949 **
Larkin, Johor (Urban)	Dependent parameter: PM_{10} Independent parameter: NO_2	0.0204 *
	Dependent parameter: PM_{10} Independent parameter: CO	0.0173 *
	Dependent parameter: PM_{10} Independent parameter: RH	0.0048 *
	Dependent parameter: O_3 Independent parameter: PM_{10}	0.0179 *
	Dependent parameter: O_3 Independent parameter: NO_2	0.0015 *
	Dependent parameter: O_3 Independent parameter: RH	0.0013 *
	Dependent parameter: CO Independent parameter: NO_2	0.0052 *
	Dependent parameter: CO Independent parameter: WS	0.0236 *

Table 11. *Cont.*

Monitoring Stations	Parameters	*p*-Value
Larkin, Johor (Urban)	Dependent parameter: O_3 Independent parameter: CO	0.01018 *
Temerloh, Pahang (Sub Urban)	Dependent parameter: NO_2 Independent parameter: RH	0.0411 *
	Dependent parameter: NO_2 Independent parameter: AT	0.0847 **
	Dependent parameter: O_3 Independent parameter: RH	0.0689 **
	Dependent parameter: CO Independent parameter: NO_2	0.0521 **
Balok Baru Kuantan, Pahang (Industry)	Dependent parameter: PM_{10} Independent parameter: NO_2	0.0292 *
Kuala Terengganu, Terengganu (Urban)	Dependent parameter: SO_2 Independent parameter: O_3	0.0013 *
	Dependent parameter: SO_2 Independent parameter: WS	0.0183 *
	Dependent parameter: NO_2 Independent parameter: PM_{10}	0.0183 *
	Dependent parameter: NO_2 Independent parameter: RH	0.0047 *
	Dependent parameter: O_3 Independent parameter: PM_{10}	0.0178 *
	Dependent parameter: CO Independent parameter: PM_{10}	0.0412 *

* *p*-value < 0.05: A *p*-value less than 0.05 is considered statistically significant. This means there is strong evidence to reject the null hypothesis (which stated there is no causal relationship between the variables). In causality studies, this would suggest a significant causal relationship between the variables. ** *p*-values between 0.05 and 0.10, suggesting moderate significance.

In suburban areas, meteorological factors showed significant influence on pollutant levels. Batu Pahat exhibited strong relationships between ambient temperature and ozone (O_3), and moderate relationships between SO_2 and NO_2. In Temerloh, Granger testing showed that relative humidity influenced NO_2 and moderately influenced O_3, while temperature moderately influenced NO_2. These findings aligned with previous research by highlighting the crucial role of temperature and humidity in shaping suburban air quality dynamics, particularly in ozone formation and nitrogen dioxide levels [18–20].

Industrial areas displayed distinct pollutant interaction patterns. Pengerang showed bidirectional causality between SO_2 and PM_{10}, with wind speed also influencing the SO_2 level. In Balok Baru Kuantan, Granger testing showed that NO_2 significantly influenced PM_{10}. These results were consistent with studies that underscored the complex interactions between gaseous pollutants and particulate matter in industrial settings, as well as the importance of meteorological factors like wind in pollutant dispersion [21–23].

Urban areas exhibited complex multi-pollutant interactions. In Larkin, Granger testing showed that NO_2 and CO influenced PM_{10}, while relative humidity influenced both PM_{10} and O_3. Kuala Terengganu showed diverse relationships: O_3 influenced SO_2, wind speed affected SO_2, and PM_{10} influenced NO_2, O_3, and CO. These findings aligned with previous research that highlighted the intricate air pollution dynamics in urban environments, characterized by multiple causal relationships between pollutants and meteorological factors [24,25].

This research makes a crucial contribution to environmental science and air quality management by thoroughly analyzing air pollution trends in Malaysia over five years, offering deep insights into the region's air quality dynamics. By using Granger causality analysis, it goes beyond mere correlations to reveal the intricate cause-and-effect relationships between air pollutants and weather conditions. The findings provide a solid foundation for creating evidence-based policies and health interventions, improving air quality forecasts, and enabling timely actions to protect public health and enhance environmental quality in Malaysia.

4. Conclusions

This study provides valuable insights into the complex relationships between air pollutants and meteorological parameters across different regions in Malaysia. Through comprehensive trend analysis and Granger causality testing, this research revealed the distinct patterns of parameter interaction in urban, suburban, and industrial areas. The findings highlighted the significant influence of temperature and humidity on ozone and nitrogen dioxide levels in suburban areas, the intricate interplay between gaseous pollutants and particulate matter in industrial settings, and the complex multi-pollutant dynamics in urban environments. These results have important implications for air quality management and urban planning in Malaysia. By understanding the causal relationships between pollutants and meteorological factors, policymakers and environmental agencies can develop more targeted and effective strategies to mitigate air pollution. This research contributes to the broader goal of improving air quality and public health in rapidly developing regions, aligning with global sustainability objectives.

Author Contributions: Conceptualization, N.R. and W.Y.P.; methodology, Z.A.R.; software, N.M.N.; validation, N.R., A.Z.U.-S. and H.A.H.; formal analysis, W.Y.P.; investigation, Z.A.R.; resources, N.R.; data curation, Z.A.R.; writing—original draft preparation, W.Y.P.; writing—review and editing, N.R.; visualization, M.K.N.M.; supervision, N.M.N.; project administration, N.R.; funding acquisition, N.R. All authors have read and agreed to the published version of the manuscript.

Funding: This research was funded by the Ministry of Higher Education Malaysia (MoHE), grant number (FRGS/1/2023/TK08/UNIMAP/02/24).

Institutional Review Board Statement: Not applicable.

Informed Consent Statement: Not applicable.

Data Availability Statement: Data are contained within the article.

Acknowledgments: This research was supported by the Ministry of Higher Education Malaysia (MoHE) through the Fundamental Research Grant Scheme (FRGS/1/2023/TK08/UNIMAP/02/24). We also want to thank to the Department of Environment (DOE) Malaysia for granting access to the comprehensive and detailed datasets, and the Mining and Energy Resources Academy (MERA) for the consultancy that was essential to the project.

Conflicts of Interest: The authors declare no conflicts of interest.

References

1. Shaziayani, W.N.; Ul-Saufie, A.Z.; Ahmat, H.; Al-Jumeily, D. Coupling of quantile regression into boosted regression trees (BRT) technique in forecasting emission model of PM10 concentration. *Air Qual. Atmos. Health* **2021**, *14*, 1647–1663. [CrossRef]
2. Shafie, S.H.M.; Mohamad, S.; Rameli, N.L.F.; Pasaribu, S.B. Analysis of urban air pollution and the effectiveness of air pollution control policy in Malaysia: Case study in Klang Valley, Malaysia. *J. Cita Huk.* **2021**, *9*, 13–28. [CrossRef]
3. Vu, T.V.; Shi, Z.; Cheng, J.; Zhang, Q.; He, K.; Wang, S.; Harrison, R.M. Assessing the impact of clean air action on air quality trends in Beijing using a machine learning technique. *Atmos. Chem. Phys.* **2019**, *19*, 11303–11314. [CrossRef]

4. Yang, X.; Wang, S.; Zhang, W.; Zhan, D.; Li, J. The impact of anthropogenic emissions and meteorological conditions on the spatial variation of ambient SO_2 concentrations: A panel study of 113 Chinese cities. *Sci. Total Environ.* **2017**, *584–585*, 318–328. [CrossRef]
5. Onwuna, D.B.; Stanley, H.O.; Abu, G.O.; Immanuel, O.M. Air quality at artisanal crude oil refinery sites in Igia-Ama, Tombia Kingdom, Rivers State, Nigeria. *Asian J. Adv. Res. Rep.* **2022**, *16*, 74–83. [CrossRef]
6. Liu, C.; Wang, H.; Ma, Q.; Ma, J.; Wang, Z.; Liang, L.; Xu, W.; Zhang, G.; Zhang, X.; Wang, T.; et al. Efficient Conversion of NO to NO_2 on SO_2-Aged MgO under Atmospheric Conditions. *Environ. Sci. Technol.* **2020**, *54*, 11848–11856. [CrossRef]
7. Janse, R.J.; Hoekstra, T.; Jager, K.J.; Zoccali, C.; Tripepi, G.; Dekker, F.W.; van Diepen, M. Conducting correlation analysis: Important limitations and pitfalls. *Clin. Kidney J.* **2021**, *14*, 2332–2337. [CrossRef]
8. Phylactou, P.; Papadatou-Pastou, M.; Konstantinou, N. The Bayesian One-sample *t*-Test Supersedes Correlation Analysis as a Test of Validity. *PsyArXiv* **2022**. [CrossRef]
9. Dong, X.; Xu, J.; Bu, Y.; Zhang, C.; Ding, Y.; Hu, B.; Ding, Y. Beyond correlation: Towards matching strategy for causal inference in Information Science. *J. Inf. Sci.* **2021**, *48*, 735–748. [CrossRef]
10. Zhang, S.; Zhou, L.; Jia, L.; Li, J.; Liu, B.; Yuan, Y. Numerical Simulation on Particulate Matter Emissions from a Layer House during Summer in Northeast China. *Atmosphere* **2022**, *13*, 435. [CrossRef]
11. Sobieraj, M.; Setny, P. Granger Causality Analysis of Chignolin folding. *J. Chem. Theory Comput.* **2022**, *18*, 1936–1944. [CrossRef] [PubMed]
12. Yashavanth, B.S.; Singh, K.N.; Paul, A.K. An agricultural price forecasting model under nonstationarity using functional coefficient autoregression. *J. Appl. Nat. Sci.* **2016**, *8*, 50–54. [CrossRef]
13. Engle, R.F.; Granger, C.W.J. Co-Integration and error correction: Representation, estimation, and testing. *Econometrica* **1987**, *55*, 251. [CrossRef]
14. Sandal, M.; Cemrek, F. Investigation of structural breaks for major stocks in the world. *Int. J. Acad. Res. Bus. Soc. Sci.* **2019**, *9*, 21–36. [CrossRef]
15. Liu, P.; Lee, H.-S. Foreign direct investment (FDI) and economic growth in China: Vector autoregressive (VAR) analysis. *SHS Web Conf.* **2020**, *80*, 01002. [CrossRef]
16. Shojaie, A.; Fox, E.B. Granger Causality: A review and recent advances. *Annu. Rev. Stat. Appl.* **2022**, *9*, 289–319. [CrossRef]
17. Raffee, A.F.; Hamid, H.A.; Rahmat, S.N.; Jaffar, M.I. The cause-and-effect analysis of ground level ozone (O_3), air pollutants and meteorological parameters using the causal relationship approach. *J. Eng. Res.* **2023**, *11*. [CrossRef]
18. Song, J.; Ma, M. Climate change: Linear and nonlinear causality analysis. *Stats* **2023**, *6*, 626–642. [CrossRef]
19. Ma, X.; Jia, H. Particulate matter and gaseous pollutions in three megacities over China: Situation and implication. *Atmos. Environ.* **2016**, *140*, 476–494. [CrossRef]
20. Liu, F.; Tan, Q.; Jiang, X.; Yang, F.; Jiang, W. Effects of relative humidity and $PM_{2.5}$ chemical compositions on visibility impairment in Chengdu, China. *J. Environ. Sci.* **2019**, *86*, 15–23. [CrossRef]
21. Millán-Martínez, M.; Sánchez-Rodas, D.; De La Campa, A.M.S.; Alastuey, A.; Querol, X.; De La Rosa, J.D. Source contribution and origin of PM10 and arsenic in a complex industrial region (Huelva, SW Spain). *Environ. Pollut.* **2021**, *274*, 116268. [CrossRef] [PubMed]
22. Zhang, S.; Li, D.; Ge, S.; Liu, S.; Wu, C.; Wang, Y.; Chen, Y.; Lv, S.; Wang, F.; Meng, J.; et al. Rapid sulfate formation from synergetic oxidation of SO_2 by O_3 and NO_2 under ammonia-rich conditions: Implications for the explosive growth of atmospheric $PM_{2.5}$ during haze events in China. *Sci. Total Environ.* **2021**, *772*, 144897. [CrossRef] [PubMed]
23. Leogrande, S.; Alessandrini, E.R.; Stafoggia, M.; Morabito, A.; Nocioni, A.; Ancona, C.; Bisceglia, L.; Mataloni, F.; Giua, R.; Mincuzzi, A.; et al. Industrial air pollution and mortality in the Taranto area, Southern Italy: A difference-in-differences approach. *Environ. Int.* **2019**, *132*, 105030. [CrossRef]
24. Choi, S.M.; Choi, H. Artificial Neural Network Modeling on PM_{10}, $PM_{2.5}$, and NO_2 Concentrations between Two Megacities without a Lockdown in Korea, for the COVID-19 Pandemic Period of 2020. *Int. J. Environ. Res. Public Health* **2022**, *19*, 16338. [CrossRef]
25. Xu, L.; Batterman, S.; Chen, F.; Li, J.; Zhong, X.; Feng, Y.; Rao, Q.; Chen, F. Spatiotemporal characteristics of $PM_{2.5}$ and PM_{10} at urban and corresponding background sites in 23 cities in China. *Sci. Total Environ.* **2017**, *599–600*, 2074–2084. [CrossRef]